The protein encoded by the duck plague virus UL14 gene regulates virion morphogenesis and affects viral replication

Jieyu Wan,[*,†,‡] Fangjie Li,[*,†,‡,#] Mingshu Wang,[*,†,‡,**] Anchun Cheng,[*,†,‡] Bin Tian,[*,†,‡] Qiao Yang,[*,†,‡] Ying Wu,[*,†,‡] Xumin Ou,[*,†,‡] Sai Mao,[*,†,‡] Di Sun,[*,†,‡] Shaqiu Zhang,[*,†,‡] Juan Huang,[*,†,‡] Qun Gao,[*,†,‡] XinXin Zhao,[*,†,‡] Shun Chen,[*,†,‡] Mafeng Liu,[*,†,‡] Renyong Jia,[*,†,‡] and Dekang Zhu[†,‡]

[*]*Institute of Preventive Veterinary Medicine, Sichuan Agricultural University, Wenjiang, Chengdu City, Sichuan, 611130, P.R. China;* [†]*Key Laboratory of Animal Disease and Human Health of Sichuan Province, Sichuan Agricultural University, Wenjiang, Chengdu City, Sichuan, 611130, P.R. China; and* [‡]*Avian Disease Research Center, College of Veterinary Medicine, Sichuan Agricultural University, Wenjiang, Chengdu City, Sichuan, 611130, P.R. China*

ABSTRACT To investigate the pivotal roles of the duck plague virus (**DPV**) tegument protein UL14 in viral replication, we generated 2 mutated viruses of DPV by using the bacterial artifcial chromosome system, the UL14-null mutant virus (CHv-BAC-ΔUL14) and the corresponding revertant virus (CHv-BAC-ΔUL14R). We found that the CHv-BAC-ΔUL14 viruses exhibited impaired virion morphogenesis in transmission electron microscopy (**TEM**) studies. Furthermore, CHv-BAC-ΔUL14 exhibited a plaque size reduction in duck embryo fibroblasts (**DEFs**). Finally, CHv-BAC-ΔUL14 exhibited a significant viral growth defect. Taken together, our findings suggest that DPV UL14 protein regulates viral morphogenesis for efficient viral replication.

Key words: duck enteritis virus, UL14, virion morphology, virus replication

2022 Poultry Science 101:101863
https://doi.org/10.1016/j.psj.2022.101863

INTRODUCTION

Duck viral enteritis (**DVE**) is caused by duck plague virus (**DPV**), which is an acute, febrile infectious disease that is transmitted via contact, associated with sepsis, and characterized by vascular damage, tissue hemorrhage, digestive mucosal eruptions, and lesions of lymphoid organs. Importantly, the disease spreads rapidly, with high morbidity and fatality rates. The characteristics of some DPV genes have been reported; these genes are linear, double-stranded DNA and consist of a unique long (**UL**) and a unique short (**US**) region, a unique short internal repeat (**IRS**) region and a unique short terminal repeat (**TRS**) region, which form the UL-IRS-US-TRS structure of the viral genome. The genome of the virus contains 78 ORFs; specifically, 65 and 11 ORFs are located in the UL and US regions, respectively, and ICP4/IE180 are located completely in the IRS and TRS regions (Wu et al., 2012a,b).

The protein UL14 (**pUL14**) was predicted to be a minor tegument protein that is not essential for viral replication. The UL14 protein is expressed late during infection and conserved in the family *Herpesviridae*, including *Alphaherpesvirinae, Betaherpesvirinae*, and *Gammaherpesvirinae* (Wada et al., 1999; Li et al., 2009). The UL14 protein shows varied localization patterns in infected cells and cells expressing only UL14, suggesting the possibility that it is multifunctional (Wada et al., 1999; Cunningham et al., 2000; Yamauchi et al., 2001). Several studies have reported the anti-apoptotic function of the herpes simplex virus type 2 (**HSV-2**) and bovine herpesvirus 1 (**BHV-1**) UL14 protein (Yamauchi et al., 2003; De Martino et al., 2007). Another study suggests that herpes simplex virus type (**HSV-1**) and HSV-2 pUL14 have a role in the nuclear targeting of capsids (Yamauchi et al., 2001; Yamauchi et al., 2008). Recently, an interesting report suggests that HSV-1 pUL14 and pUL51 form a stable protein−protein interaction, and the UL14-UL51 complex regulates the final viral envelopment step for efficient viral replication (Oda et al., 2016). However, there is no clear role for DPV UL14 protein.

Received January 20, 2022.
Accepted March 8, 2022.

[#]These authors contributed equally to this work as first authors.

[**]Corresponding author: mshwang@163.com

Table 1. Primers used to construct and analyze the recombinants.

Primers	Sequence	Products (bp)
ΔUL14-Kan (F)	5-ATATGATTTGTTTTTTC CTACTCTATT GAATAGTGCG CACTCTCGCT AAC GTGTAGGCTGGAGCTGCTTC-3	Kan gene fanked by of UL14
ΔUL14-Kan (R)	5-TCCGATAGGATTCATTTCGCTAATAGGGCTTCGTCGTCT TCGTCCAGCCA CATATGAATATCCTCCTTAG-3	
ΔUL14R-UL14(F)	5-CTGCAATACGGACTATTTTATACAGCAAGTGTAAGTAGAT ATATGGGGTA GTGTAGGCTGGAGCTGCTTC-3	UL14 fragment with homoloy
ΔUL14RUL14(R)	5-ATGCGACTATGTTTGTGTTACATATGAATATCCTCCTTAG-3	
ΔUL14R- Kan (F)	5-CTAAGGAGGATATTCATATG TAACACAAAC ATAGTCGCAT-3	Kan fragment with right homoloy arm of UL14
ΔUL14R- Kan (R)	5-TCCGATAGGATTCATTTCGCTAATAGGGCTTCGTCGTCTT CGTCCAGCCA-3	
UL14 (F)	5-TATTTGCAATGTATGT-3	UL14 gene identifcation primers
UL14 (R)	5-CACCGGATCCGAGGAA-3	
qPCR1	5-TTTTCCTCCTCGCTGAGT-3	
qPCR1	5-GGCCGGGTTTGCAGAAGT-3	
qPCR ((probe)	5-CCCTGGGTACAAGCG-3	

Note: F (forward primer); R (reverse primer). - indicates the homologous arms; ~ indicates the Kan fragments.

Therefore, we focused on the function of the DPV tegument protein pUL14. Using a two-step Red recombination system implemented on the DPV CHv genome cloned into a bacterial artificial chromosome to delete the UL14 gene. Electron microscopy analysis indicated that the virion was irregular. Deletion of UL14 significantly reduced the viral titers and plaque sizes of DPV in infected cells. Our results show firstly that the DPV UL14 protein affects viral replication by regulating viral morphogenesis and viral cell-to-cell spread, which will provide a reference for research on the function of the UL14 protein.

MATERIALS AND METHODS

Virus and Cells

The previously reported DEV CHv strain (GenBank No. JQ647509) and parental virus (**CHv-BAC**) were preserved in our laboratory (Zhao et al., 2008; Chang et al., 2009). Duck embryo fibroblasts (**DEFs**) were harvested from 8-day-old duck embryos and grown in minimum essential medium (**MEM;** Gibco-BRL, Grand Island, NY) supplemented with 10% newborn bovine serum (**NBS;** Gibco-BRL, Grand Island, NY). Anti-UL14 polyclonal antibodies were all generated in our laboratory.

Construction of CHv-BAC Mutant and Revertant Viruses

The CHv-BAC-ΔUL14 and CHv-BAC-ΔUL14R recombinant viruses were constructed as described previously (Ma et al., 2018). In brief, a linear PCR fragment containing a kanamycin resistance (**kanR**) gene flanked on both sides by the UL14 sequence was amplified from the pKD4 vector with the indicated primers. Second, positive clones were electroporated into DH10B cells containing the pBAC-DPV clone and pKD46, with the help of Exo, Beta, and Gam recombinase, replacing the UL14 ORF. Subsequently, the KanR gene was removed. The kanR-containing clone was cultured at 42°C to cure pKD46, and pCP20 was electroporated to induce recombination between 2 FRT sites. The positive bacteria were identified by PCR using identification primers and confirmed by sequencing. For the construction of the revertant mutant, the procedure was almost the same, except for the kanR gene flanking regions, which were expanded with the designed primers. The correctly sequenced plasmid was transfected into DEFs, producing the CHv-BAC-ΔUL14 and CHv-BAC-ΔUL14R viruses. Both viruses were confirmed by PCR and Western blotting to ensure the deletion and expression of UL14. The forward and reverse primers used in this step are listed in Table 1.

Western Blot

Samples were separated by 12% sodium dodecyl sulfate-polyacrylamide gel electrophoresis (**SDS-PAGE**) and transferred onto nitrocellulose membranes (**PVDF**, Millipore, Boston, MA). Subsequently, the membranes were blocked for 2 h in 5% skim milk at 37°C, incubated with primary antibody, and incubated with HRP-conjugated secondary antibody (Bio-Rad, Hercules, CA) for 1 h at 37°C. Finally, the protein signal was visualized with an enhanced chemiluminescence (**ECL**) Western blotting analysis system. The following antibodies were used: a rabbit anti-UL14 polyclonal antibody (1:200) and a mouse anti-GAPDH antibody (Abmart, Shanghai, China, 1:5000).

Fluorescent Quantitative Real-Time PCR

The total DNA extraction and fluorescent quantitative real-time PCR(**FQ-PCR**) analysis procedures were described previously (Guo et al., 2009).

Viral Adsorption, Penetration, Replication, and Release Assays

For viral adsorption, DEFs were cultured in 12-well plates, prechilled at 4°C for 1 h, and infected with a

0.001 MOI of CHv-BAC, CHv-BAC-ΔUL14, and CHv-BAC-ΔUL14R virus. The cells infected with viruses were incubated at 4°C for an additional 2 h, washed 3 times with ice-cold phosphate-buffered saline (**PBS**), covered with 1.5% methylcellulose, incubated at 37°C under 5% CO_2 for 72 h, and counted via a plaque assay. For viral penetration, DEFs were cultured in 12-well plates, prechilled at 4°C for 1 h, and infected with a 0.001 MOI of CHv-BAC, CHv-BAC-ΔUL14, and CHv-BAC-ΔUL14R virus. Subsequently, the viruses were allowed to penetrate for 2 h at 4°C, and the cells were washed 3 times with ice-cold PBS, added to 2% NBS medium with cultivation in a CO_2 incubator at 37°C for 3 h, washed with ice-cold PBS 3 times, covered with 1.5% methylcellulose, incubated at 37°C under 5% CO_2 for 72 h, and counted via a plaque assay. For viral replication, DEFs were infected with CHv-BAC, CHv-BAC-ΔUL14, and CHv-BAC-ΔUL14R viruses at an MOI of 1 for 6 h, incubated at 37°C under 5% CO_2, and incubated in 2% NBS medium at 37°C under 5% CO_2. The infected cells were collected at 7, 8, and 9 h. The infected cells were collected, and total DNA was isolated following the manufacturer's instructions. DNA was quantified by real-time PCR. To determine the role of UL14 on DPV release, DEFs were infected with the CHv-BAC, CHv-BAC-ΔUL14, and CHv-BAC-ΔUL14R viruses at an MOI of 1 for 18 h, and 2% NBS medium was added, and the cells were incubated at 37°C under 5% CO_2. The cell supernatant was harvested at 30, 60, 90,and 120 min, and the $TCID_{50}$ was determined. Three independent experiments were performed in triplicate (He et al., 2021).

Plaque Morphology

To investigate the effect of DPV UL14 protein on cell-to-cell transmission, a virus plaque assay was carried out. The DEFs were infected with a 0.001 MOI of CHv-BAC, CHv-BAC-ΔUL14, and CHv-BAC-ΔUL14R virus, and the viruses were allowed to penetrate for 2 h at 37°C in 5% CO_2. The virus solution was discarded, the cells were washed 3 times with PBS, and MEM medium containing 1% methylcellulose was added. After culture in a CO_2 incubator at 37°C for 4 to 5 days, the pathological changes of the cells were observed with a microscope, 4% paraformaldehyde was added to fix the cells at 4°C for 2 h, and the 4% paraformaldehyde was discarded. The cells were washed 3 times with PBS, stained with 1% crystal violet for 5 min at room temperature, rinsed repeatedly with PBS, and plaques were observed and counted.

Electron Microscopy

The ultrastructural morphology of virions within infected cells was examined by TEM. DEFs were infected with 10^5 $TCID_{50}$ of the CHv-BAC, CHv-BAC-ΔUL14, and CHv-BAC-ΔUL14R viruses. After 36 h, the DEFs were washed with PBS and fixed with 2.5% glutaraldehyde at 4°C for 2 h. The cells were scraped and centrifuged at 5,000 r/min for 3 min at 4°C; the supernatant was discarded, and the cells were centrifuged at 40,000 r/min for 2 h. The cells were then fixed in 2.5% glutaraldehyde again, washed 3 times with PBS, fixed in 1.0% osmium tetroxide for 1 h and then subjected to stepwise dehydration in acetone. The cells were embedded in epoxy resin and polymerized at 80°C for 72 h. Ultrathin sections (80 nm) were prepared by the standard method, stained with 1% uranyl acetate for 20 min and 1% lead citrate for 20 min, and examined with an H-600 transmission electron microscope.

Determination of Genome Copy Numbers and Growth Kinetics

To investigate the effect of UL14 protein on the number of viral genomes during viral replication, real-time quantitative PCR was performed. Briefly, the DEFs in the 12-well plates were cultured in a CO_2 incubator at 37°C for 12 h. DEFs in 6-well plates were infected with the CHv-BAC, CHv-BAC-ΔUL14, and CHv-BAC-ΔUL14R viruses at an MOI of 1. Samples of the infected cells and their supernatants were collected at 6, 12, 24, 48, 72, and 84 hours and frozen at −20°C for later use. After three repeated freezing and thawing cycles, the cells were fully lysed to release the virus, and the virus obtained from the supernatant and the precipitate was diluted 10 times. The viral genome was extracted according to the phenol-chloroform method. Then the genomes were quantified by qPCR with probe primers of UL30.

Statistical Analysis

Comparisons between the different groups were made by one-way ANOVA with GraphPad Prism 8.0 software (La Jolla, CA). The data was expressed as the mean ± standard deviation (**SD**) of 3 independent experiments. Asterisks indicate the level of statistical significance ($^{*}P < 0.05$; $^{**}P < 0.01$; $^{***}P < 0.001$; $^{****}P < 0.0001$).

RESULTS

Construction and Identification of Recombinant Viruses

To characterize the functions of DPV UL14 protein, CHv-BAC-ΔUL14 (Δ1-425 bp) and CHv-BAC-ΔUL14R viruses were constructed using a 2-step Red recombination mutagenesis system as described in the Materials and Methods (Figure 1A). Recombinant viruses were identified by restriction fragment length polymorphism (**RFLP**) analysis and DNA sequencing (data not shown). Specifically, the BAC DNA of recombinant virus extracted from the clones identified

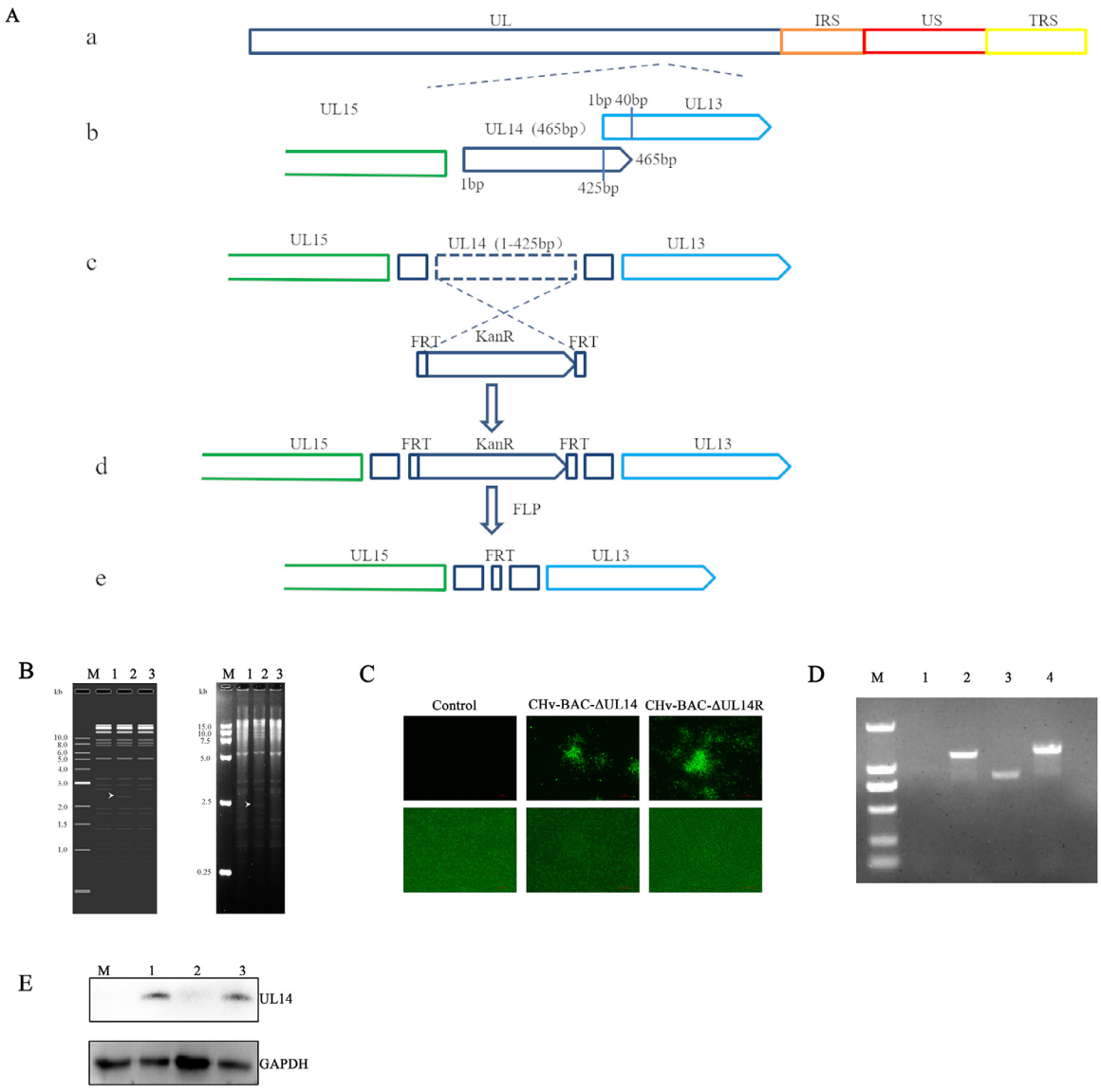

Figure 1. Construction and identification of recombinant viruses. (A) Schematic diagram of DPV CHv-BAC-ΔUL14 construction. (a) The DPV genome consists of unique long (UL), unique short (US), internal repeat (IR) and terminal repeat (TR) regions. (b) Partial UL14 region. (c-d) The UL14 ORF replaced by kanR. (d) KanR deletion via the Flp-FRT recombination system. (B) Restriction fragment length polymorphism analysis of recombinant virus. Orientation and real gel analysis of DPV CHv-BAC (Lane 1), DPV CHv-BAC-ΔUL14 (Lane 2) and DPV CHv-BAC-ΔUL14R (Lane 3) digested by BamHI. Asterisks indicate the different bands, and the image on the left was obtained by software simulation. (C) Rescue of the DPV CHv-BAC-ΔUL14 and DPV CHv-BAC-UL14R recombinant viruses. Green fluorescent plaques and the corresponding cells were observed at 6 d after transfection. (magnification: 100×; scale bar: 10 μm). (D) Identification of recombinant viruses by PCR analysis. 2,000 bp marker (M) is shown as a reference. Lanes: 1, Mock; 2, CHv-BAC; 3, CHv-BAC-ΔUL14; 4, CHv-BAC-ΔUL14R. (E) Western blot analysis of pUL14 expression in cells infected with recombinant viruses. The pUL14 band was detected in the DPV CHv-BAC and DPV CHv-BAC-UL41R groups but not in the mock or DPV CHv-BAC-ΔUL14 groups. GAPDH was used as the loading control.

by PCR was single-enzyme digested with *Bam*HI for RFLP analysis. The results showed that the restriction patterns of the *Bam*HI digestion products of DPV CHv-BAC, DPV CHv-BAC-ΔUL14, CHv-BAC, and CHv-BAC-ΔUL14R were the same as predicted (Figure 1B). Combined with sequencing, these results showed that no unnecessary mutations were generated (data not shown), indicating that infectious clones containing CHv-BAC-ΔUL14 and CHv-BAC-ΔUL14R were successfully constructed.

The plasmid with the correct sequence was transfected into DEFs to obtain the viruses CHv-BAC-ΔUL14 and CHv-BAC-ΔUL14R (Figure 1C). Furthermore, the BAC DNA of the recombinant virus was extracted for PCR analysis. The bands from CHv-BAC and CHv-BAC-ΔUL14R were approximately 1301 bp and 1217 bp, respectively, and those from CHv-BAC-ΔUL14 were approximately 792 bp (Figure 1D). In addition, the primers used in this experiment are shown in Table 1.

According to the Western blot results, CHv-BAC and CHv-BAC-ΔUL14R expressed UL14 protein with a band at approximately 17.5 kDa, and CHv-BAC-ΔUL14 failed to express UL14 protein (Figure 1E). Taken

together, these results suggest that the DPV CHv-BAC-ΔUL14 mutant and DPV CHv-BAC-UL41R revertant viruses were constructed successfully.

The DPV pUL14 is Involved in Viral Morphogenesis

To investigate the role of UL14 protein in DPV life cycle, we next examined the effects of UL14 protein on the adsorption, penetration, DNA replication and viral morphogenesis processes. As shown in Figure 2 (A, B, C), viral adsorption, penetration and DNA replication were similar among the viruses. These results showed that deletion of the UL14 gene did not significantly affect virus adsorption, penetration or DNA replication.

Next, we investigated whether viral morphogenesis was affected by UL14. The viral ultrastructural morphology was observed by using TEM. During the proliferation of DPV, capsid assembly occurs in the nucleus. In the electron micrographs shown in Figure 3(A-a, B-b, C-c), these particles were similar in structure, and the electron-dense core was wrapped in capsids in the nuclei of cells infected with CHv-BAC, CHv-BAC-ΔUL14, or CHv-BAC-ΔULR. These results indicated that the UL14 protein did not affect the assembly of viral DNA in the capsid.

The final envelopment steps of DPV occurred in the cytoplasm, and mature virions were transported out of the cell via entry into a vesicle. As shown in Figure 3(D-d, F-f), viral particles were complete and regular were observed in DEFs infected with CHv-BAC or CHv-BAC-ΔUL14R; however, viral particles with an incomplete envelope were observed in DEFs infected with CHv-BAC-ΔUL14 (Figure 3E-e). These results indicated that the UL14 protein played an important role in viral morphogenesis in the cytoplasm.

Virus particles outside the cell have a mature structure. Analysis of the extracellular virion structure can explain the role of the UL14 protein in the structural morphogenesis of virion. As shown in Figure 3(G-g, I-i), structure of the viral particles released from cells was complete and regular, and the electron density was high in DEFs infected with CHv-BAC or CHv-BAC-ΔUL14R. In contrast, irregular structures and low electron density were observed in DEFs infected with CHv-BAC-ΔUL14 (Figure 3H-h). These results indicated that UL14 played an important role in the morphogenesis of the virus particle structure.

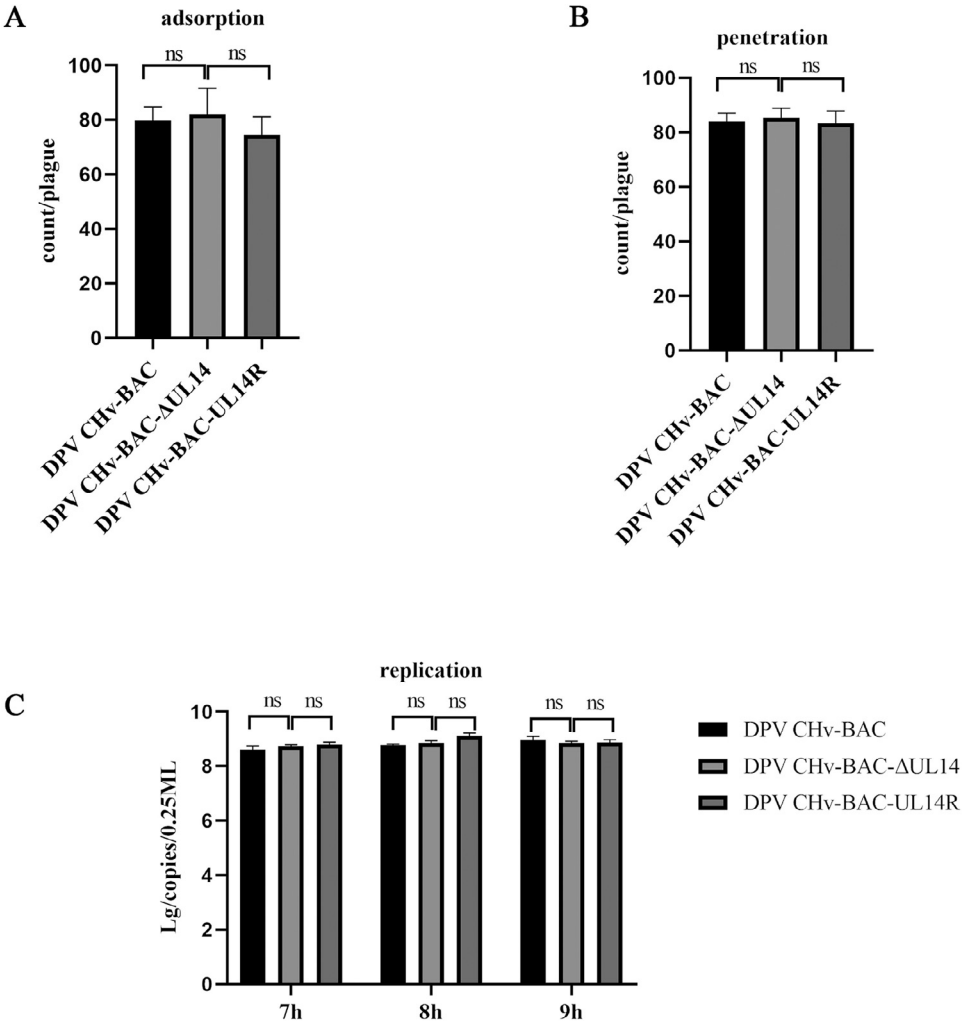

Figure 2. Effect of UL14 on virus replication. The role of the DPV UL14 gene in the viral life cycle: adsorption (A), penetration (B), and replication (C). The data were analyzed by one-way ANOVA.

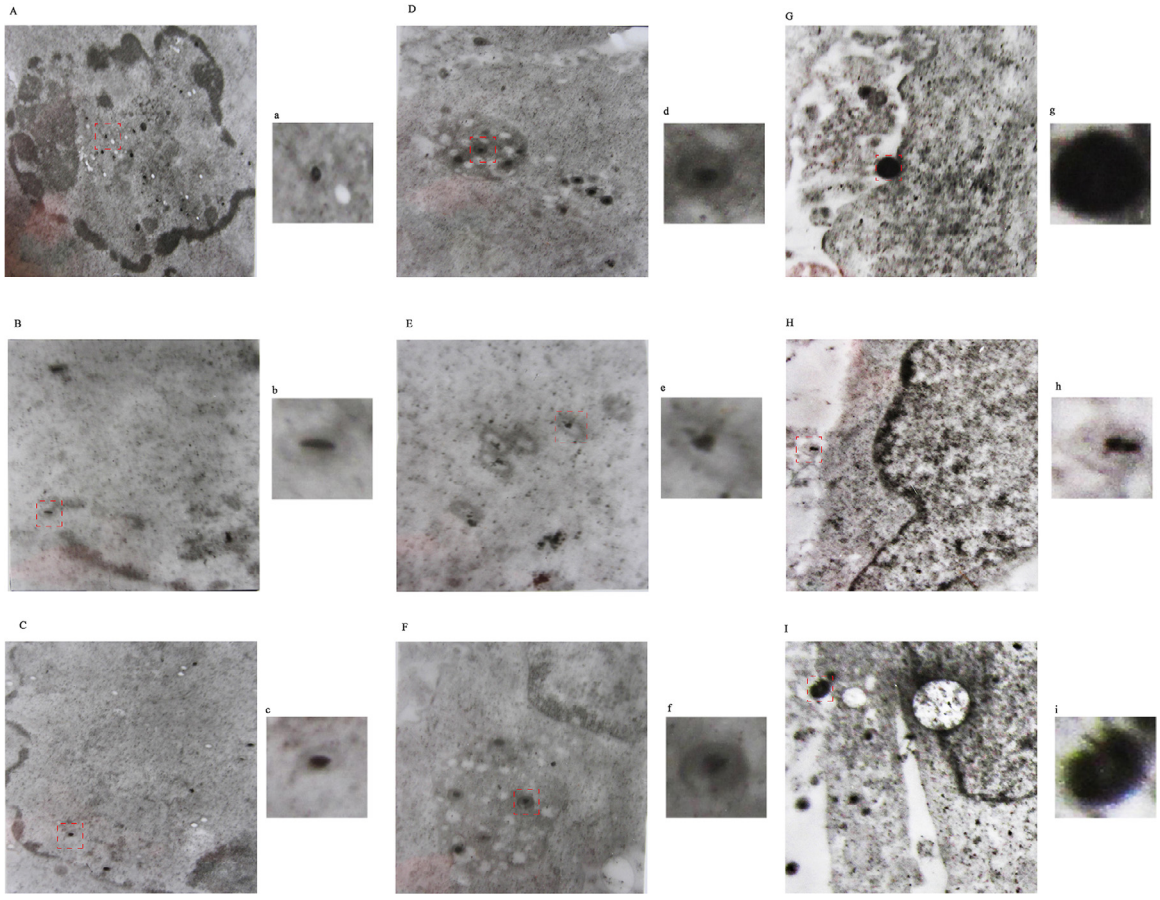

Figure 3. Ultrastructural morphologies of recombinant viruses. DEFs were infected with 10^5 $TCID_{50}$ of DPV CHv-BAC, DPV CHv-BAC-ΔUL14 and DPV CHv-BAC-UL14R and examined by electron microscopy. A, B, and C show nucleocapsids in the nucleus for CHv-BAC (A-a), CHv-BAC-ΔUL14 (B-b), and CHv-BAC-UL14R (C-c). These particles were similar in structure. The electron-dense core were wrapped in capsid. (A, B, C 200,000×). D, E, and F show viral particles in the cytoplasm. CHv-BAC (D-d), CHv-BAC-ΔUL14 (E-e), CHv-BAC-UL14R (F-f). There were viral particles with an incomplete envelope in cells infected with DPV CHv-BAC-ΔUL14. (D, E, F 400,000×). G, H, and I show viral particles released from cells. CHv-BAC (G-g), CHv-BAC-ΔUL14 (H-h), CHv-BAC-UL14R (I-i). (G, H, I 400,000×). The red boxed areas in the central images are enlarged in the insets on the left.

DPV pUL14 is Involved in Virus Release and Spread

The UL14 mutation resulted in a clear defect in viral morphogenesis. Therefore, we expected to find a similar defect in viral release and spread with the CHv-BAC-ΔUL14 virus. As shown in Figure 4, compared with the DPV CHv-BAC parent and DPV CHv-BAC-UL14R revertant viruses, deletion of the UL14 gene significantly inhibited viral release.

We next explored the effects of the DPV UL14 protein on transmission between adjacent cells with plaque morphology assays. As shown in Figure 5 (A, B), the DPV CHv-BAC and DPV CHv-BAC-UL14R recombinant viruses produced plaques that were similar in size individually and on average. However, the plaques produced by the DPV CHv-BAC-ΔUL14 mutant viruses were smaller than those produced by the parental and revertant viruses. At the same time, we also detected viral plaques using crystal violet staining. As shown in

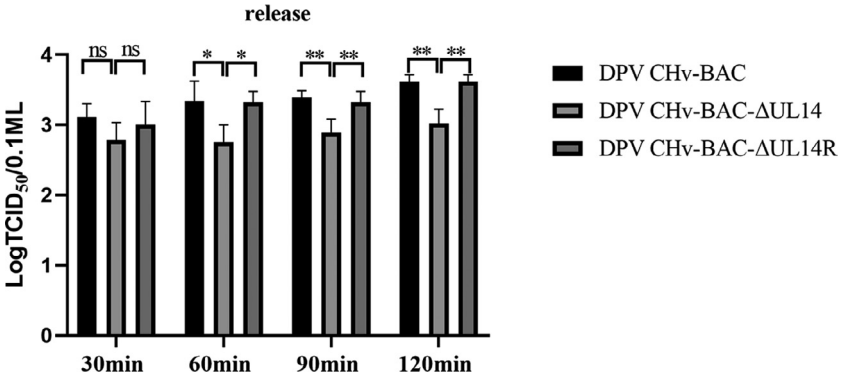

Figure 4. Deletion of the UL14 gene inhibits viral release. The data were analyzed by one-way ANOVA. $^*P < 0.1$,$^{**}P < 0.01$.

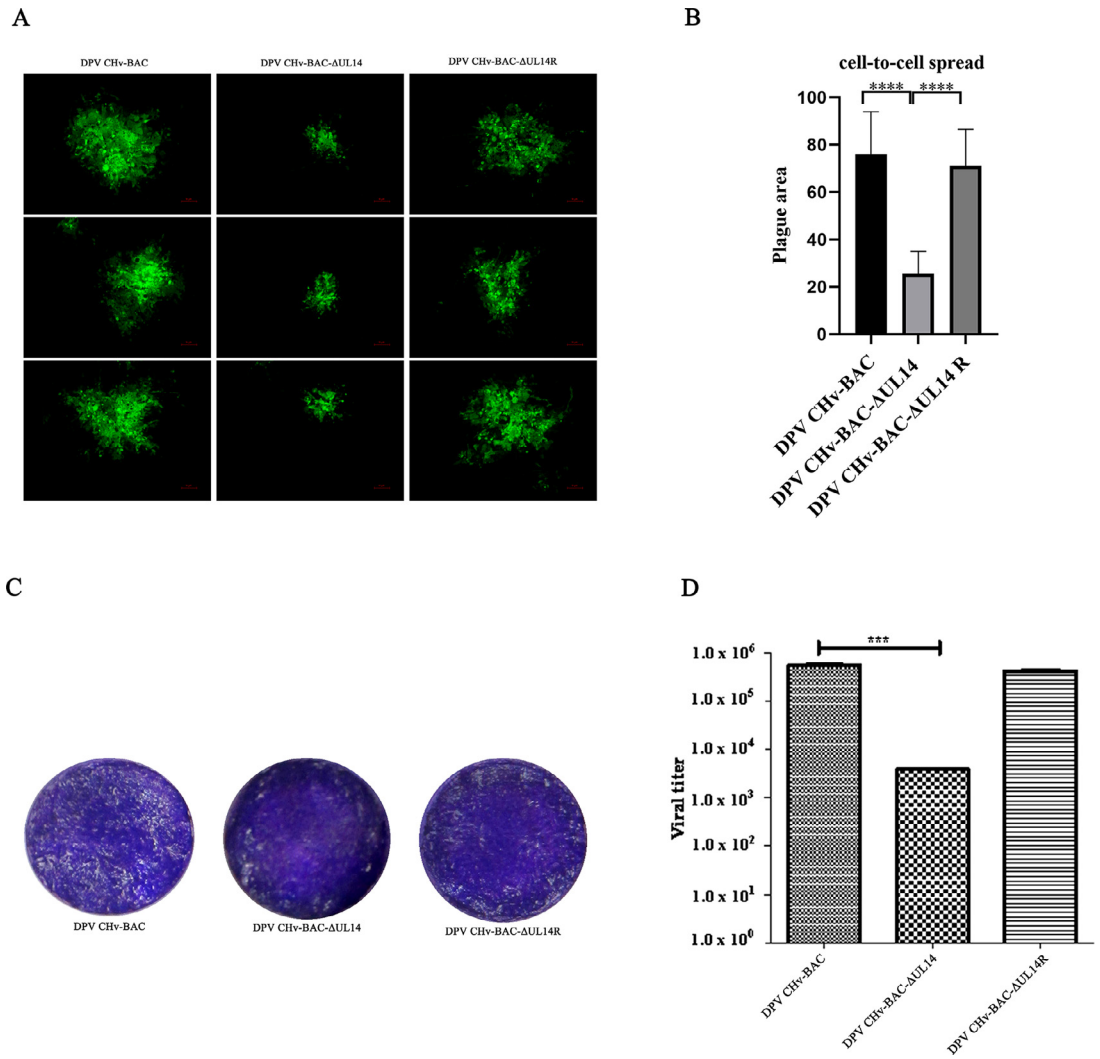

Figure 5. Plaque morphologies of recombinant viruses. DEFs in 12-well plates were infected with an MOI of 0.001 of the DPV CHv-BAC, DPV CHv-BAC-ΔUL14, and DPV CHv-BAC-UL14R recombinant viruses. After incubation at 37°C for 2 h, the infected cells were covered with 1.5% methylcellulose and cultured. (A) Green fluorescent plaques produced by the three recombinant viruses. (B) Statistical analysis of thirty different randomly selected viral green fluorescent plaques. The data were analyzed by one-way ANOVA. $^{****}P < 0.0001$. (magnification: 100×; scale bar: 10 μm). (C) Images of viral plaques after 1.0% crystal violet staining. (D) Statistical analysis of thirty different randomly selected viral plaques with crystal violet staining. $^{***}P < 0.001$.

Figure 5(C, D), the UL14 deletion mutant still produced smaller viral plaques than the parental and revertant viruses. There was little difference in plaque size between the parental and revertant viruses; in contrast, the titer of the UL14-deleted mutant virus was significantly lower than that of the parental and revertant viruses. These

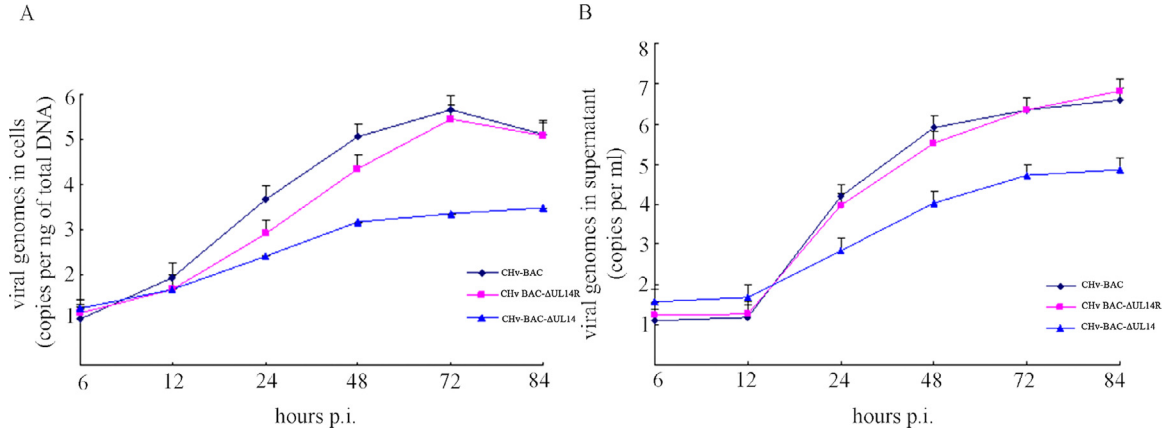

Figure 6. Kinetics of infectious virus production in supernatant and cells after infection with DPV CHv-BAC, DPV CHv-BAC-ΔUL14, and DPV CHv-BAC-UL14R at an MOI of 1. (A) The viral genome copy numbers in infected cells. (B) The viral genome copy numbers in the supernatant.

data indicated that the DPV UL14 protein influenced viral cell-to-cell spread.

DPV pUL14 is Involved in Viral Multistep Growth Kinetics

To investigate the role of UL14 in viral replication, DEFs were infected with the DPV CHv-BAC, DPV CHv-BAC-ΔUL14, and DPV CHv BAC-ΔUL14R viruses at an MOI of 1. The genome was extracted as a template, UL30 primers were used as measurement primers, and quantitative PCR with the probe method was used for absolute quantitative analysis. The results showed that the copy number of the virus genome for the CHv-BAC-ΔUL14 virus was significantly lower than those for the CHv-BAC and CHv-BAC-ΔUL14 viruses. The supernatant and pellet genome copy number changes were roughly the same (Figure 6A, B). These results indicated that UL14 deletion impaired virus replication.

DISCUSSION

In previous studies, HSV-2 UL14 was shown to play a role in viral assembly and maturation by promoting translocation of the minor capsid protein VP26, DNA cleavage and packaging of the UL33 protein in the nucleus (Yamauchi et al., 2001). Our study did not report these effects of UL14 on VP26 and UL33; however, in DEFs infected with CHv-BAC or CHv-BAC-ΔUL14R, the structure of viral particles released from cells was complete and regular, and the electron density was high (Figure 3G-g, I-i). In contrast, irregular structures and low electron density were seen in DEFs infected with CHv-BAC-ΔUL14 (Figure 3H-h). Our analysis indicated that DPV UL14 played an important role in the morphogenesis of the virus particle structure.

The generation of mutant viruses with a defect in the morphogenesis of the virus particle structure allowed us to determine the impacts of this defect on viral spread and release. Several studies have shown that there are 2 ways for alpha herpes viruses to enter cells: cell-free infection and cell-to-cell spread (Hubner et al., 2009; Jin et al., 2009; Zhao et al., 2017). Notably, the cell-to-cell spread of viruses facilitates rapid viral dissemination and immune evasion (Mothes et al., 2010). Earlier studies showed that a mutant with a UL14 deletion generated small plaques after infection of HSV-1 cells (Cunningham et al., 2000). Furthermore, previous studies on DPV indicated that duck plague virus glycoprotein I influenced cell-cell spread and that US3 had a similar function (Deng et al., 2020; Liu et al., 2020). In our study, we found that the UL14 deletion mutant still produced smaller viral plaques and lower viral titers (Figure 5). These results indicate that DPV UL14 also affected virus release and cell-cell spread.

Previous studies indicated that HSV-1 UL14 regulated the expression of immediate-early genes by enhancing VP16 nuclear localization (Yamauchi et al., 2008; Ohta et al., 2011). Some studies have suggested that murine gamma virus 68 (MHV-68) ORF34, a homolog of HSV-1 pUL14, stimulates late gene expression by recruiting the transcription initiation complex (Wu et al., 2009). Additionally, a mutant virus with HSV-1 UL14 deletion exhibited an extended growth cycle at a low multiplicity of infection (Cunningham et al., 2000). In our results, viral DNA generation, as indicated by the number genome copies, by the UL14 deletion mutant was significantly lower than that of the parental and revertant viruses from 12 to 84 hpi (Figure 6). These results indicate that the UL14 deletion mutant virus showed decreased extracellular virus yields in multistep growth kinetics experiments.

In summary, in this study, we found that the DPV UL14 protein affected viral replication by regulating viral morphogenesis and viral cell-to-cell spread, which will provide a reference for research on the function of the UL14 protein.

ACKNOWLEDGMENTS

This work was supported by the China Agriculture Research System of MOF and MARA, and the Sichuan Veterinary Medicine and Drug Innovation Group of China Agricultural Research System (SCCXTD-2020-18).

DISCLOSURES

The authors declare that they have no conflict of interest.

REFERENCES

Chang, H., A. Cheng, M. Wang, Y. Guo, W. Xie, and K. Lou. 2009. Complete nucleotide sequence of the duck plague virus gE gene. Arch. Virol. 154:163–165.

Cunningham, C., A. J. Davison, A. R. MacLean, N. S. Taus, and J. D. Baines. 2000. Herpes simplex virus type 1 gene UL14: phenotype of a null mutant and identification of the encoded protein. J. Virol. 74:33–41.

De Martino, L., G. Marfe, M. I. Consalvo, C. Di Stefano, U. Pagnini, and P. Sinibaldi-Salimei. 2007. Antiapoptotic activity of bovine herpesvirus type-1 (BHV-1) UL14 protein. Vet. Microbiol. 123:210–216.

Deng, L., M. Wang, A. Cheng, Q. Yang, Y. Wu, R. Jia, S. Chen, D. Zhu, M. Liu, X. Zhao, S. Zhang, J. Huang, X. Ou, S. Mao, L. Zhang, Y. Liu, Y. Yu, B. Tian, L. Pan, M. U. Rehman, and X. Chen. 2020. The pivotal roles of US3 protein in cell-to-cell spread and virion nuclear egress of duck plague virus. Sci Rep 10:7181.

Guo, Y., A. Cheng, M. Wang, C. Shen, R. Jia, S. Chen, and N. Zhang. 2009. Development of TaqMan MGB fluorescent real-time PCR assay for the detection of anatid herpesvirus 1. Virol. J. 6:71.

He, T., M. Wang, A. Cheng, Q. Yang, R. Jia, Y. Wu, J. Huang, B. Tian, M. Liu, S. Chen, X. X. Zhao, D. Zhu, S. Zhang, X. Ou, S. Mao, Q. Gao, and D. Sun. 2021. DPV UL41 gene encoding protein induces host shutoff activity and affects viral replication. Vet. Microbiol. 255:108979.

Hubner, W., G. P. McNerney, P. Chen, B. M. Dale, R. E. Gordon, F. Y. Chuang, X. D. Li, D. M. Asmuth, T. Huser, and

B. K. Chen. 2009. Quantitative 3D video microscopy of HIV transfer across T cell virological synapses. Science 323:1743–1747.

Jin, J., N. M. Sherer, G. Heidecker, D. Derse, and W. Mothes. 2009. Assembly of the murine leukemia virus is directed towards sites of cell-cell contact. PLoS Biol. 7:e1000163.

Li, Y., B. Huang, X. Ma, J. Wu, F. Li, W. Ai, M. Song, and H. Yang. 2009. Molecular characterization of the genome of duck enteritis virus. Virology 391:151–161.

Liu, T., M. Wang, A. Cheng, R. Jia, Q. Yang, Y. Wu, M. Liu, X. Zhao, S. Chen, S. Zhang, D. Zhu, B. Tian, M. U. Rehman, Y. Liu, Y. Yu, L. Zhang, L. Pan, and X. Chen. 2020. Duck plague virus gE serves essential functions during the virion final envelopment through influence capsids budding into the cytoplasmic vesicles. Sci Rep 10:5658.

Ma, Y., Q. Zeng, M. Wang, A. Cheng, R. Jia, Q. Yang, Y. Wu, X. X. Zhao, M. Liu, D. Zhu, S. Chen, S. Zhang, Y. Liu, Y. Yu, L. Zhang, and X. Chen. 2018. US10 protein is crucial but not indispensable for duck enteritis virus infection in vitro. Sci. Rep. 8:16510.

Mothes, W., N. M. Sherer, J. Jin, and P. Zhong. 2010. Virus cell-to-cell transmission. J. Virol. 84:8360–8368.

Oda, S., J. Arii, N. Koyanagi, A. Kato, and Y. Kawaguchi. 2016. The interaction between herpes simplex virus 1 tegument proteins UL51 and UL14 and its role in virion morphogenesis. J. Virol. 90:8754–8767.

Ohta, A., Y. Yamauchi, Y. Muto, H. Kimura, and Y. Nishiyama. 2011. Herpes simplex virus type 1 UL14 tegument protein regulates intracellular compartmentalization of major tegument protein VP16. Virol. J. 8:365.

Wada, K., F. Goshima, H. Takakuwa, H. Yamada, T. Daikoku, and Y. Nishiyama. 1999. Identification and characterization of the UL14 gene product of herpes simplex virus type 2. J. Gen. Virol. 80:2423–2431.

Wu, T. T., T. Park, H. Kim, T. Tran, L. Tong, D. Martinez-Guzman, N. Reyes, H. Deng, and R. Sun. 2009. ORF30 and ORF34 are essential for expression of late genes in murine gammaherpesvirus 68. J. Virol. 83:2265–2273.

Wu, Y., A. Cheng, M. Wang, Q. Yang, D. Zhu, R. Jia, S. Chen, Y. Zhou, X. Wang, and X. Chen. 2012a. Complete genomic sequence of Chinese virulent duck enteritis virus. J. Virol. 86:5965.

Wu, Y., A. Cheng, M. Wang, D. Zhu, R. Jia, S. Chen, Y. Zhou, and X. Chen. 2012b. Comparative genomic analysis of duck enteritis virus strains. J. Virol. 86:13841–13842.

Yamauchi, Y., T. Daikoku, F. Goshima, and Y. Nishiyama. 2003. Herpes simplex virus UL14 protein blocks apoptosis. Microbiol. Immunol. 47:685–689.

Yamauchi, Y., K. Kiriyama, N. Kubota, H. Kimura, J. Usukura, and Y. Nishiyama. 2008. The UL14 tegument protein of herpes simplex virus type 1 is required for efficient nuclear transport of the alpha transinducing factor VP16 and viral capsids. J. Virol. 82:1094–1106.

Yamauchi, Y., K. Wada, F. Goshima, H. Takakuwa, T. Daikoku, M. Yamada, and Y. Nishiyama. 2001. The UL14 protein of herpes simplex virus type 2 translocates the minor capsid protein VP26 and the DNA cleavage and packaging UL33 protein into the nucleus of coexpressing cells. J. Gen. Virol. 82:321–330.

Zhao, F., T. Zhao, L. Deng, D. Lv, X. Zhang, X. Pan, J. Xu, and G. Long. 2017. Visualizing the essential role of complete virion assembly machinery in efficient Hepatitis C virus cell-to-cell transmission by a viral infection-activated split-intein-mediated reporter system. J. Virol. 91:e01720–16.

Zhao, L., A. Cheng, M. Wang, G. Yuan, and M. Cai. 2008. Characterization of codon usage bias in the dUTPase gene of duck enteritis virus. Prog. Nat. Sci. 18:1069–1076.